Journal of Alloys and Compounds 509 (2011) 6950–6954

Contents lists available at ScienceDirect

Journal of Alloys and Compounds

journal homepage: www.elsevier.com/locate/jallcom

$CuInSe_2$ nano-crystallite reaction kinetics using solid state reaction from Cu_2Se and In_2Se_3 powders

Hsing-I Hsiang*, Li-Hsin Lu, Yu-Lun Chang, Dahtong Ray, Fu-Su Yen

Department of Resources Engineering, Particulate Materials Research Center, National Cheng Kung University, Tainan 70101, Taiwan, ROC

ARTICLE INFO

Article history:
Received 28 September 2010
Received in revised form 1 April 2011
Accepted 1 April 2011
Available online 8 April 2011

Keywords:
$CuInSe_2$
Cu_2Se
In_2Se_3
Kinetics
Solid state reaction

ABSTRACT

The reaction mechanism and $CuInSe_2$ formation kinetics using a solid state reaction from Cu_2Se and In_2Se_3 powders synthesized using a heating up process were investigated using X-ray diffractomy (XRD) and transmission electron microscopy (TEM). It was observed that the $CuInSe_2$ phase increased gradually, accompanied with a decrease in γ-In_2Se_3 with no intermediate phase as the calcination temperature and soaking time were increased. The reaction kinetics was analyzed using the Avrami and polynomial kinetic model, suggesting that $CuInSe_2$ formation from Cu_2Se and In_2Se_3 powders follows a diffusion-controlled reaction with an apparent activation energy of about 122.5–182.3 kJ/mol. Cu_2Se and In_2Se_3 phases react and directly transform into CIS without the occurrence of any intermediate phase and the size of the newly formed $CuInSe_2$ crystallites was close to that of the Cu_2Se reactant particle based on the TEM results, which indicated that the solid reaction kinetics may be dominated by the diffusion of In^{3+} ions.

1. Introduction

I-III-VI chalcopyrite thin film solar cells were developed to improve the conversion efficiency and reduce the cost over more than ten years. $CuInSe_2$ (CIS) is one of the most important semiconductor materials used in thin film photovoltaic cells. The conventional vacuum processes for CIS have many shortcomings such as high production cost and difficulty in scaling up [1,2]. Therefore, developing colloidal routes, such as spin-casting or printing, to fabricate CIS thin film solar cells that have well controlled stoichiometry, high materials utilization and low processing equipment cost have attracted much attention [3]. $CuInSe_2$ (CIS) powder has been reported successfully synthesized using solid-state reaction [4–8], solvo-thermal [9–12], thermolysis [13] and thermal decomposition methods [14–17]. Compared to the liquid-phase process, the solid state reaction is much easier and cheaper. However, CIS powders prepared using solid state reactions reported by previous studies have many drawbacks, such as larger crystallite size or lower chemical purity [4–8]. This leads to CIS powders prepared using the conventional solid state reaction unsuitable for application in wet processing to fabricate CIS thin film solar cells. To date, previous studies on the reaction mechanism and kinetics of CIS formation concentrated primarily on the bilayer In_2Se_3/CuSe precursor films [18–21]. Kim et al. [18] investigated the reaction mechanism and kinetics of CIS formation from bilayer In_2Se_3/CuSe precursor films and suggested that the reaction follows a one-dimensional diffusion controlled reaction with an activation energy of 162 kJ/mol dominated by Cu diffusion. Park et al. [21] investigated the mechanism and kinetics of CIS formation during In_2Se_3/Cu_2Se inter-diffusion reaction and observed the CIS phase formed within Cu_2Se grains and at the Cu_2Se grain boundaries, indicating that CIS formation is dominated by In^{3+} diffusion. This suggests that there are still many unclear points involved in the CIS formation reaction mechanism. The reaction mechanism and kinetics of CIS formation from Cu_2Se and In_2Se_3 powders have not been reported to our best knowledge.

This study presents CIS nano-crystals successfully synthesized using solid-state reaction with the help of newly available very fine starting materials (Cu_2Se and In_2Se_3 powders synthesized using a heating process). The reaction mechanism and kinetics of $CuInSe_2$ formation using solid state reaction from Cu_2Se and In_2Se_3 powders were investigated using X-ray diffractomy (XRD) and transmission electron microscopy (TEM).

2. Experimental

2.1. Materials

Cu_2Se: Cu_2O (5.21 mmol) was readily dissolved in 10 ml condensed hydrochloric acid (HCl). After removing the redundant water, the copper chloride mixture was combined in oleylamine (OLA) (12 ml) and heated to 130 °C under an air atmosphere until the precursors were completely dissolved. Forty-five millilitres of octadecene (ODE) and 5.21 mmol of Se powder were added to a three neck flask and heated to 200 °C under an air atmosphere until completely dissolved. The metal complex (Cu–OLA) solution was then mixed and heated to 250 °C and held for 3 h.

* Corresponding author. Tel.: +886 6 2757575x62821; fax: +886 6 2380421.
E-mail address: hsingi@mail.ncku.edu.tw (H.-I. Hsiang).

0925-8388/$ – see front matter © 2011 Elsevier B.V. All rights reserved.
doi:10.1016/j.jallcom.2011.04.009

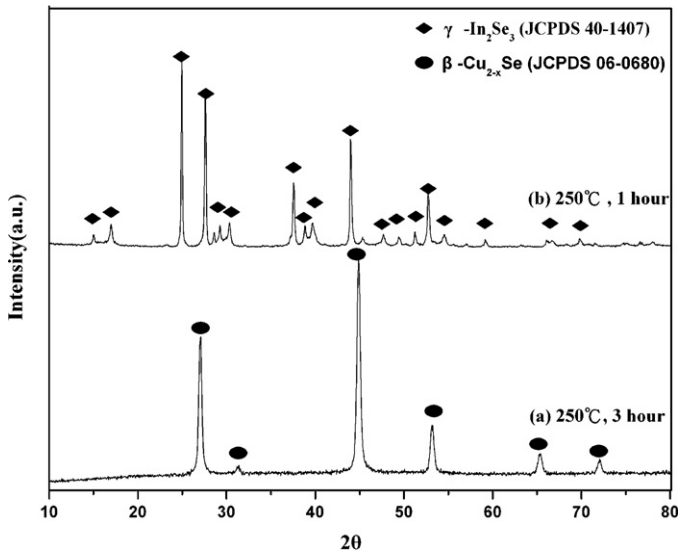

Fig. 1. XRD patterns of Cu_2Se and In_2Se_3 powders synthesized using the heating-up process.

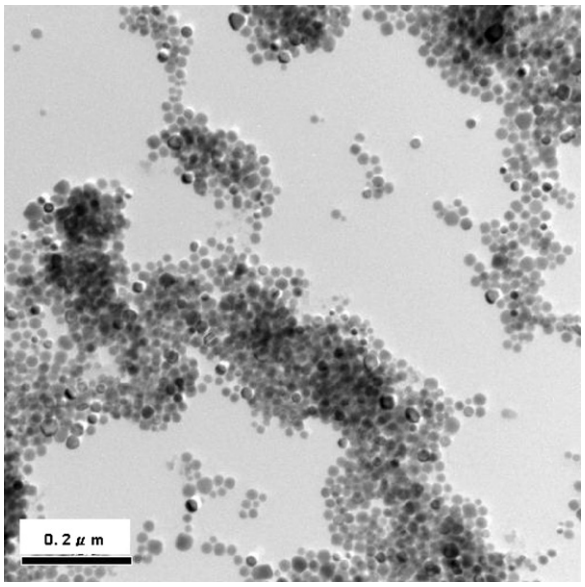

Fig. 2. TEM image of Cu_2Se crystallites.

In_2Se_3: Metal In (3.47 mmol) was dissolved in 30 ml condensed hydrochloric acid (HCl) at 150 °C and dried at 180 °C. After drying, the indium chloride was combined in OLA (12 ml) and heated to 200 °C under an air atmosphere until the precursors were completely dissolved. The mixture was then cooled to room temperature. 5.21 mmol of Se powder was dissolved using 45 ml ODE at 200 °C. The mixture was then cooled to room temperature. The two solutions were then mixed, heated and stirred at 250 °C for 1 h.

After the reaction, the mixture was cooled to 80 °C where 30 ml of ethanol was added to discontinue the reaction. This solution was then centrifuged at 6000 rpm for 5 min. The product was washed with isopropanol and n-hexane ethanol several times prior to drying at 70 °C.

2.2. Solid state reaction

For the reaction mechanism study, the mixtures were obtained directly by magnetically stirring equimolar ratios of Cu_2Se and In_2Se_3 powders synthesized using the heating process in an n-hexane solution for 12 h. The solution was then vacuum-dried at 40 °C for 6 h. The obtained dried mixtures were then calcined at different temperatures.

2.3. Materials characterization

The crystalline phases were characterized using an X-ray diffractometer (Dandong Fangyuan, DX-2700, Sandong, China) with Cu Kα radiation. The scan range was from 15° to 70° with a scan step of 0.04° and a scan rate of 2.5°/min. Transmission electron microscopy (HTEM, Hitachi HF-2000) and scanning electron microscopy (SEM, Hitachi S4100) with an attached EDS system (Noran, Voyager 1000, Waltham, MA) were used to observe the morphology, crystallite size and composition. Differential scanning calorimetry (DSC) analysis was performed using a thermal analysis instrument (Netzsch STA, 409 PC, Burlington, MA) under 40 ml/min N_2 flow rate.

3. Results and discussion

The XRD patterns of Cu_2Se and In_2Se_3 powders synthesized using the heating-up process are shown in Fig. 1. The figure indicates that the pure β-Cu_2Se (JCPDS 06-0680) and γ-In_2Se_3 (JCPDS 40-1407) can be obtained using the heating-up process. The TEM image of Cu_2Se crystallites is shown in Fig. 2. This suggests that nearly mono-dispersed spherical Cu_2Se crystallites with a size of about 20 nm can be obtained at 250 °C for 3 h using the heating-up process. Fig. 3 shows the SEM image of γ-In_2Se_3 crystallites. It indicates that the γ-In_2Se_3 crystallites exhibit a hexagonal shape with crystallite sizes of 0.5–2 μm. The Cu_2Se crystallite size was much smaller than that of γ-In_2Se_3. This can be explained as follows. In our previous study, the $CuIn_{0.7}Ga_{0.3}Se_2$ formation mechanism was investigated. It was observed that the OLA–copper complex was decomposed and released monomers containing Cu^+ ions at a lower reaction temperature for a shorter period compared to OLA–In complex because the OLA–copper complex reactivity is much higher than that of OLA–In complex. When the OLA–copper complex was heated, nucleation started and a large number of nuclei formed due to its high reactivity. Therefore, there were fewer residual monomers and the monomer supply in the growth stage could not afford a quick growth. Conversely, when the OLA–In complex was heated, nucleation was difficult due to its high bond strength. The indium monomer consumption was very low during nucleation. As a result, a higher growth rate was obtained for γ-In_2Se_3 crystallite because a large amount of the indium monomer remained after nucleation.

Figs. 4–6 show the XRD patterns of mixtures calcined at 310–330 °C for different periods. The figures demonstrate that the Cu_2Se and In_2Se_3 phases react and directly transform into CIS without any intermediate phase. As the reaction time was prolonged, the γ-In_2Se_3 phase gradually disappeared, while the CIS phase gradually increased. As the temperature was raised, the γ-In_2Se_3 phase disappeared and CIS phase increased significantly.

Fig. 7 shows the γ-In_2Se_3 fraction consumption as a function of time at different calcination temperatures. It indicates that the Cu_2Se and In_2Se_3 phases reacted at temperatures above 310 °C and γ-In_2Se_3 consumption increased with increasing soaking time and calcination temperature. The solid-state reaction kinetics between

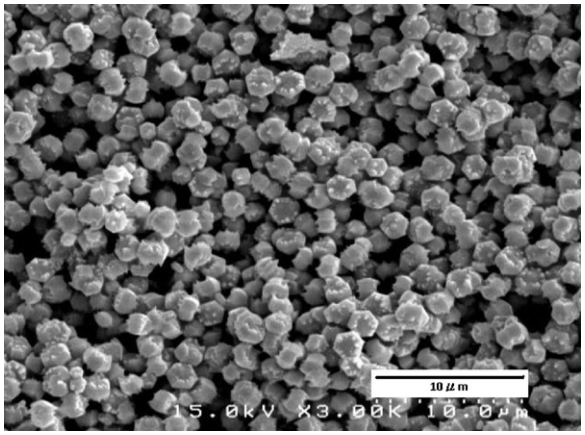

Fig. 3. SEM image of γ-In_2Se_3 crystallites.

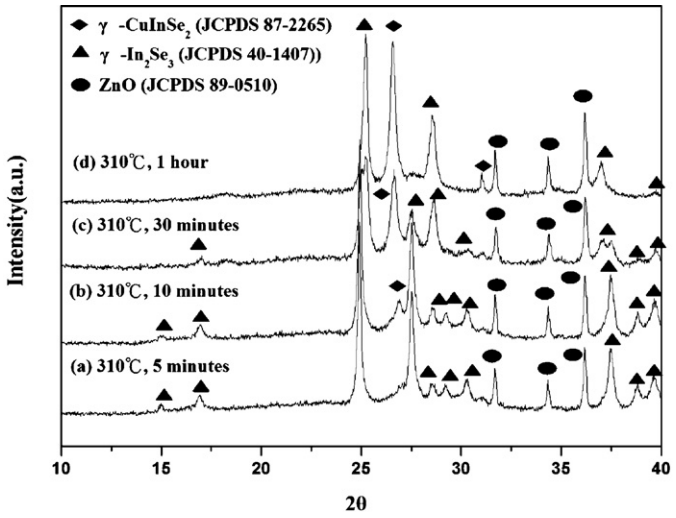

Fig. 4. XRD patterns of the mixtures calcined at 310 °C for different periods (ZnO: internal standard).

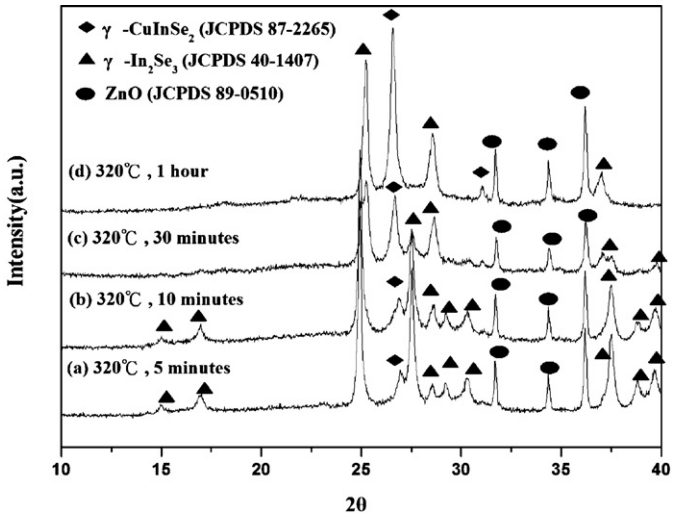

Fig. 5. XRD patterns of the mixtures calcined at 320 °C for different periods (ZnO: internal standard).

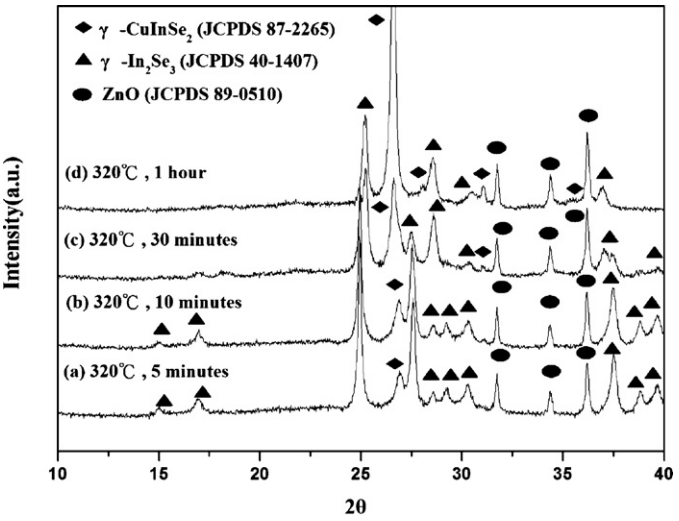

Fig. 6. XRD patterns of the mixtures calcined at 330 °C for different periods (ZnO: internal standard).

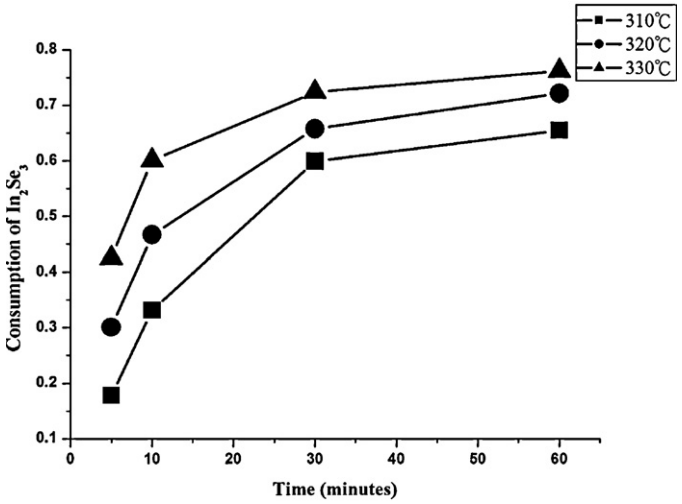

Fig. 7. Consumption fraction of γ-In_2Se_3 as a function of time at different calcination temperatures.

Cu_2Se and In_2Se_3 were investigated using two solid state reaction models, the Avarami and polynomial rate model. Fig. 8 shows a plot of $\ln(-\ln(1-y))$ vs. $\ln t$ with a regression line fitted, where y is the CIS mole fraction. The slope provides the Avrami exponent, n. Moreover, the linear fitting intercept represents the kinetic constant, k(T). According to the Arrehenius equation, the activation energy (E_a) for γ-In_2Se_3 consumption can be determined from the $\ln k$ vs. $1/T$ slope plot in Fig. 9. The Avrami exponent, n, is about 0.5, suggesting that the reaction is dominantly controlled by one-dimensional diffusion. The activation energy for this reaction is about 122.5 kJ/mol.

The polynomial kinetic model can be described by $y = kt^n$, where y is the CIS mole fraction, k is the kinetic rate constant, t is the reaction time and n is the time exponent. A linear regression analysis of CIS formation as a function of calcination time was performed to determine the best fit n values:

$$\ln y = \ln k + n \ln t$$

Fig. 10 shows a plot of $\ln y$ vs. $\ln t$ with a regression line fitted. The n values for 310, 320, and 330 °C are 0.22, 0.35, and 0.53, respectively, which suggest that the reaction is dominantly controlled by bulk diffusion [22]. This can be explained by the fact that CIS formation becomes increasingly more difficult as the CIS phase grows because the constituent elements must diffuse through

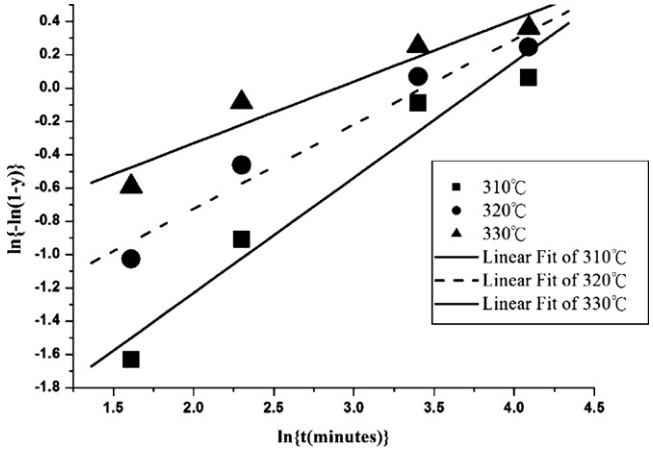

Fig. 8. Plots of $\ln(-\ln(1-y))$ vs. $\ln t$ for specimens calcined at different temperatures.

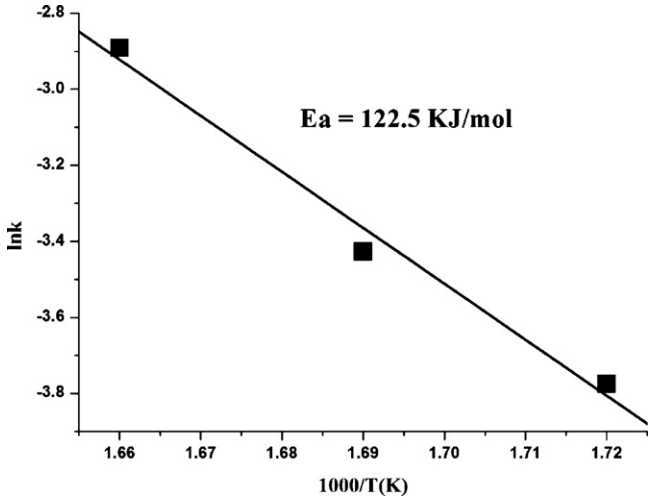

Fig. 9. Arrhenius plot for the CIS formation.

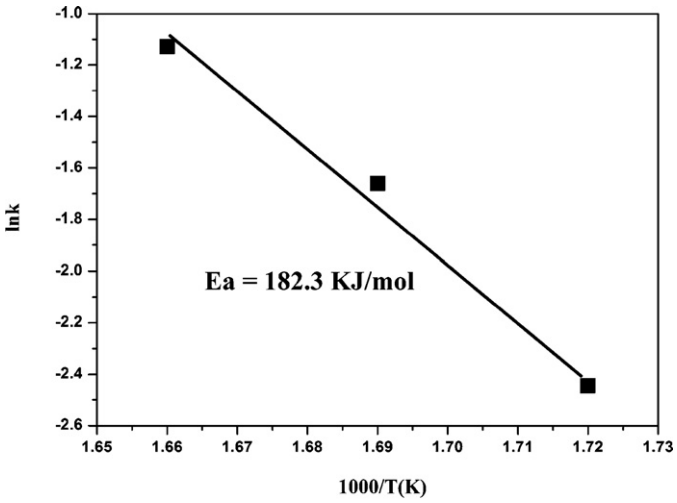

Fig. 11. Arrhenius plot of $\ln k$ vs. $1/T$ for the polynomial kinetic model.

the product phase to reach the reaction site. For the case of ideal diffusion kinetics, the n value is 0.5. However, the subparabolic growth kinetics ($n < 0.5$) was obtained for temperatures of 310 °C and 320 °C. This may be because the derivation of parabolic growth relationships assumes molar volume constancy within the system. The absence of molar volume constancy for CIS formation using solid state reaction from Cu_2Se and In_2Se_3 powders [4] is most likely responsible for growth rates which appear to be subparabolic [22]. Fig. 11 shows the Arrhenius plot of $\ln k$ vs. $1/T$ for the polynomial kinetic model. The apparent activation energy is found to be about 182.3 kJ/mol. The estimated activation energy is close to a value of about 162 kJ/mol using In_2Se_3 and CuSe as the raw materials reported by Kim et al. [19].

Connor et al. [23] found that the conversion from Cu_2S to $CuInS_2$ required little lattice distortion and thus can be done with a low energy barrier due to (1) sulfur sublattice sharing by the hexagonal Cu_2S and $CuInS_2$ and (2) In^{3+} ions can easily replace Cu^+ distributed in the interstitial sites formed by the S sublattice. Park et al. [21] investigated CIS phase formation during Cu_2Se/In_2Se_3 interdiffusion reaction and observed that In^{3+} was the fast component in diffusion through Cu_2Se, following ionic lattice diffusion through the Cu vacancy sites of Cu_2Se phase and the β and γ-phases were obtained near the In_2Se_3 phase side resulting from Cu^+ ions diffusion toward the In_2Se_3 phase. In this study, Cu_2Se and In_2Se_3 phases react and directly transform into CIS without the occurrence of any intermediate phase. Moreover, the sizes of new formed CIS nano-crystallites after heat treatment are about 20 nm, which are close to that of the $Cu_{2-x}Se$ raw materials as shown in Fig. 12. These results suggest that the CIS formation kinetics may be dominated by the diffusion of In^{3+} ions.

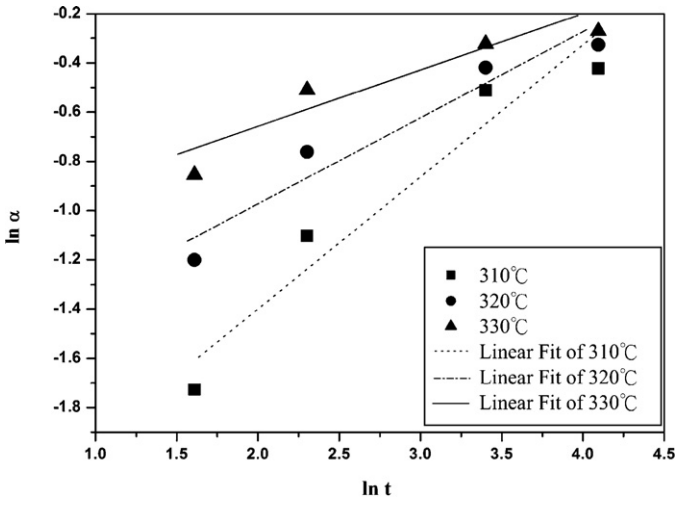

Fig. 10. A plot of $\ln y$ vs. $\ln t$ with a regression line fitted.

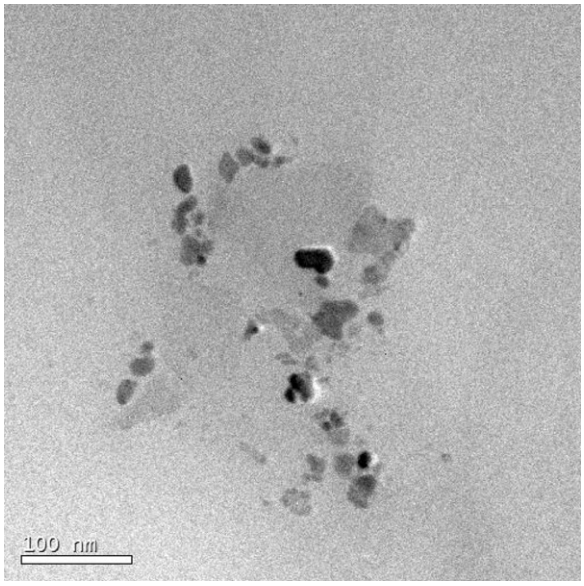

Fig. 12. TEM image of the mixture calcined at 330 °C for 30 min.

4. Conclusions

The CIS nano-crystals can be successfully synthesized using solid-state reaction with the help of fine Cu_2Se and In_2Se_3 powders synthesized using the heating-up process. The solid state reaction kinetics was analyzed using the Avrami and polynomial kinetic model, suggesting that $CuInSe_2$ formation from Cu_2Se and In_2Se_3 powders follows a diffusion-controlled reaction with an apparent activation energy of about 122.5–182.3 kJ/mol. Cu_2Se and In_2Se_3 phases react and directly transform into CIS without the occurrence of any intermediate phase and the sizes of the new-formed CIS nano-crystallites after heat treatment were about 20 nm, which were close to that of the $Cu_{2-x}Se$ raw materials. These suggest that the CIS formation kinetics may be dominated by the diffusion of In^{3+} ions.

Acknowledgment

This work was financially sponsored by the National Science Council of the Republic of China (98-2622-E-006-027-CC3).

References

[1] S.J. Ahn, K.H. Kim, K.H. Yoon, Curr. Appl. Phys. 8 (2008) 766–769.
[2] M. Kaelin, D. Rudmann, F. Kurdesau, T. Meyer, H. Zogg, A.N. Tiwari, Thin Solid Film 431–432 (2003) 58–62.
[3] D. Pan, L. An, Z. Sun, W. Hou, Y. Yang, Z. Yang, Y. Lu, J. Am. Chem. Soc. 130 (2008) 5620–5621.
[4] N. Yamamoto, S. Ishida, H. Horinaka, Jpn. J. Appl. Phys. 28 (1989) 1780–1783.
[5] T. Wada, H. Kinoshita, J. Phys. Chem. Solids 66 (2005) 1987–1989.
[6] T. Wada, Y. Matsuo, S. Nomura, Y. Nakamura, A. Miyamura, Y. Chiba, A. Yamada, M. Konagai, Phys. Stat. Sol. (A) 203 (2006) 2593–2597.
[7] S.M. Wu, Y.Z. Xue, Z.H. Zhang, J. Alloys Compd. 491 (2010) 456–459.
[8] N. Benslim, S. Mehdaoui, O. Aissaoui, M. Benabdeslem, A. Bouasla, L. Bechiri, A. Otmani, X. Portier, J. Alloys Compd. 489 (2010) 437–440.
[9] K.-H. Kim, Y.-G. Chun, B.-O. Park, K.-H. Yoon, Mater. Sci. Forum 449–452 (2004) 273–276.
[10] Y.-G. Chun, K.-H. Kim, K.-H. Yoon, Thin Solid Films 480–481 (2005) 46–49.
[11] Y.H. Yang, Y.T. Chen, J. Phys. Chem. B 110 (2006) 17370–17374.
[12] J. Olejníček, C.A. Kamler, A. Mirasano, A.L. Martinez-Skinner, M.A. Ingersoll, C.L. Exstrom, S.A. Darveau, J.L. Huguenin-Love, M. Diaz, N.J. Ianno, R.J. Soukup, Solar Energy Mater. Solar cells 94 (2010) 8–11.
[13] K.H. Kim, S.J. Ahn, B.T. Ahn, K.H. Yoon, Solid State Phenomena 124–126 (2007) 983–986.
[14] Q. Guo, S.J. Kim, M. Kar, W.N. Shafarman, R.W. Birkmire, E.A. Stach, R. Agrawal, H.W. Hillhouse, Nano Lett. 8 (2008) 2982–2987.
[15] J. Tang, S. Hinds, S.O. Kelley, E.H. Sargent, Chem. Mater. 20 (2008) 6906–6910.
[16] M.G. Panthani, V. Akhavan, B. Goodfellow, J.P. Schmidtke, L. Dunn, A. Dodabalapur, P.F. Barbara, B.A. Korgel, J. Am. Chem. Soc. 130 (2008) 16770–16777.
[17] E. Lee, J.W. Cho, J. Kim, J. Yun, J.H. Kim, B.K. Min, J. Alloys Compd. 506 (2010) 969–972.
[18] W.K. Kim, S. Kim, E.A. Payzant, S.A. Speakman, S. Yoon, R.M. Kaczynski, R.D. Acher, T.J. Anderson, O.D. Crisalle, S.S. Li, V. Craciun, J. Phys. Chem. Solids 66 (2005) 1915–1919.
[19] S. Kim, W.K. Kim, R.M. Kaczynski, R.D. Acher, S. Yoon, T.J. Anderson, O.D. Crisalle, J. Vac. Sci. Tech. 2 (2005) A 23.
[20] W.K. Kim, E.A. Payzant, S. Yoon, T.J. Anderson, J. Cryst. Growth 294 (2006) 231–235.
[21] J.S. Park, Z. Dong, S. Kim, J.H. Perepezko, J. Appl. Phys. 87 (2000) 3683–3690.
[22] A.D. Romig, Y.A. Chang, J.J. Stephens, D.R. Frear, V. Marcotte, C. Lea, in: D.R. Frear (Ed.), Solder Mechanics – A State of the Art Assessment, The Minerals, Metals and Materials Society, 1991, p. 55, Chapter 2.
[23] S.T. Connor, C.M. Hsu, B.D. Weil, S. Aloni, Y. Cui, J. Am. Chem. Soc. 131 (2009) 4962–4966.